Supporting Information for

Assembly of Chiral Cluster-Based Metal-Organic Frameworks and the Chirality Memory Effect during their Disassembly

Guocheng Deng, Boon K. Teo* and Nanfeng Zheng*

Collaborative Innovation Center of Chemistry for Energy Materials, State Key Laboratory for Physical Chemistry of Solid Surfaces, National & Local Joint Engineering Research Center of Preparation Technology of Nanomaterials, College of Chemistry and Chemical Engineering, Xiamen University, Xiamen 361005, China

*Corresponding Authors. Email: nfzheng@xmu.edu.cn, boonkteo@xmu.edu.cn

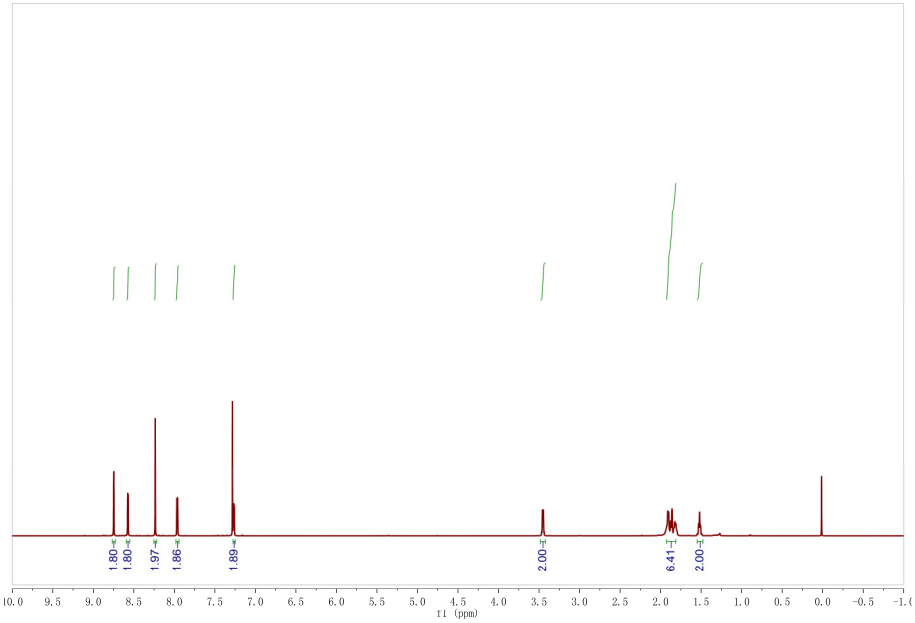

Figure S1. ^{1}H NMR spectrum of **LS** in $CDCl_3$.

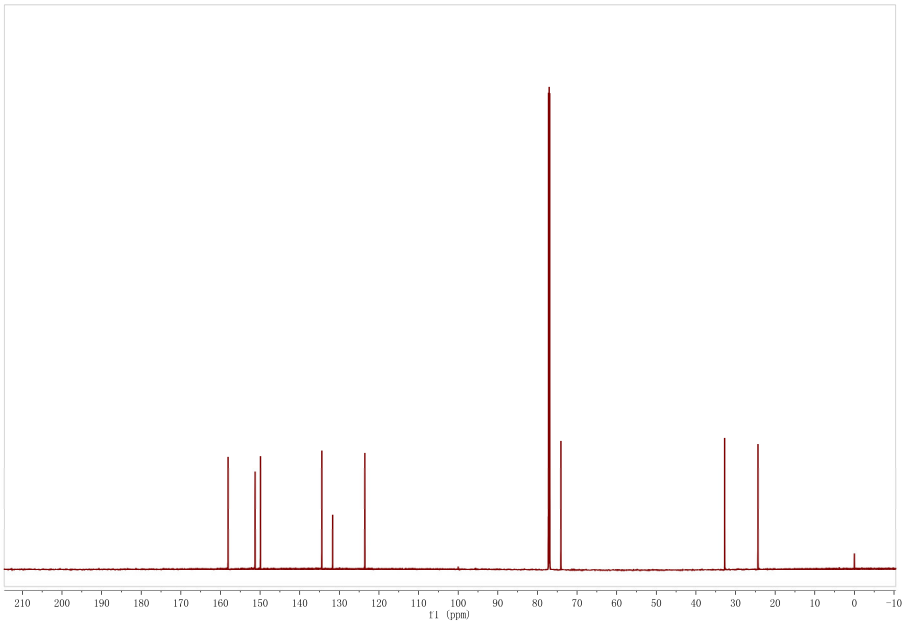

Figure S2. ^{13}C NMR spectrum of **LS** in $CDCl_3$.

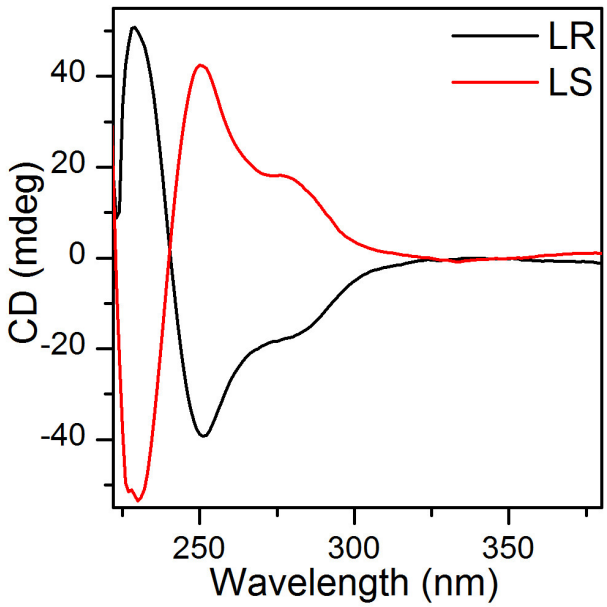

Figure S3. CD spectra of **LR** and **LS** in dichloromethane solution.

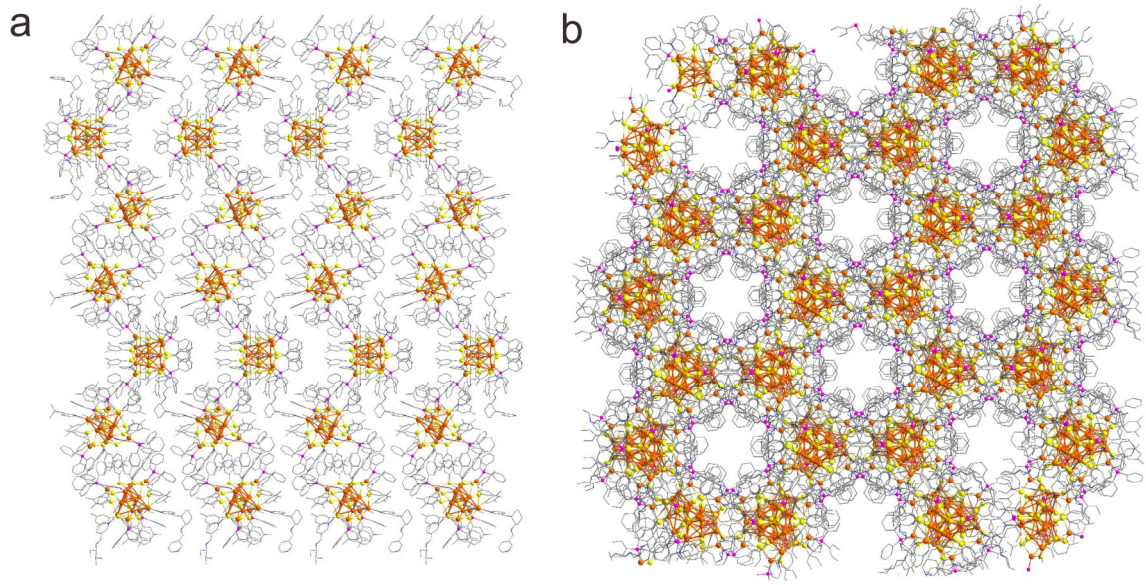

Figure S4. Crystal structure of **Ag_{14}–LS** viewed along *b* (a) and *c* axis (b). Color legend: orange sphere, Ag; yellow sphere, S; pink sphere, P; blue sphere, N; grey sphere, C. All hydrogen and fluorine atoms are omitted for clarity.

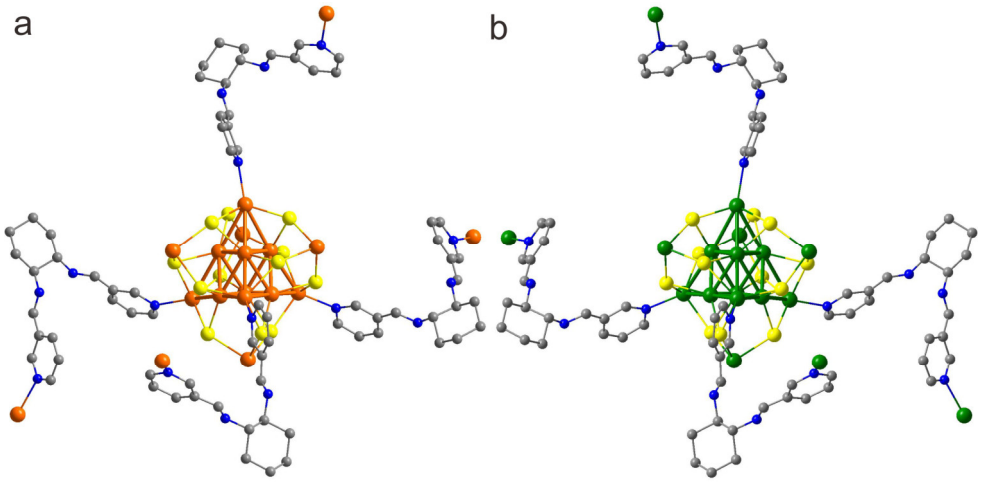

Figure S5. The structures of the building blocks of **Ag_{14}–LS** (a) and **Ag_{14}–LR** (b). Color legend: orange and green sphere, Ag; yellow sphere, S; blue sphere, N; grey sphere, C.

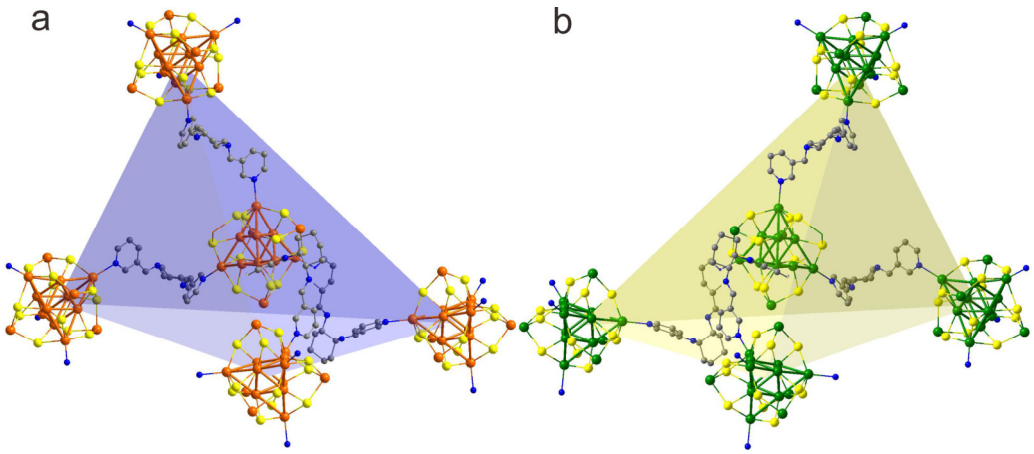

Figure S6. Distorted tetrahedron structures form by the **Ag_{14}** building blocks in **Ag_{14}-LS** (a) and **Ag_{14}-LR** (b). Color legend: orange and green sphere, Ag; yellow sphere, S; blue sphere, N; grey sphere, C.

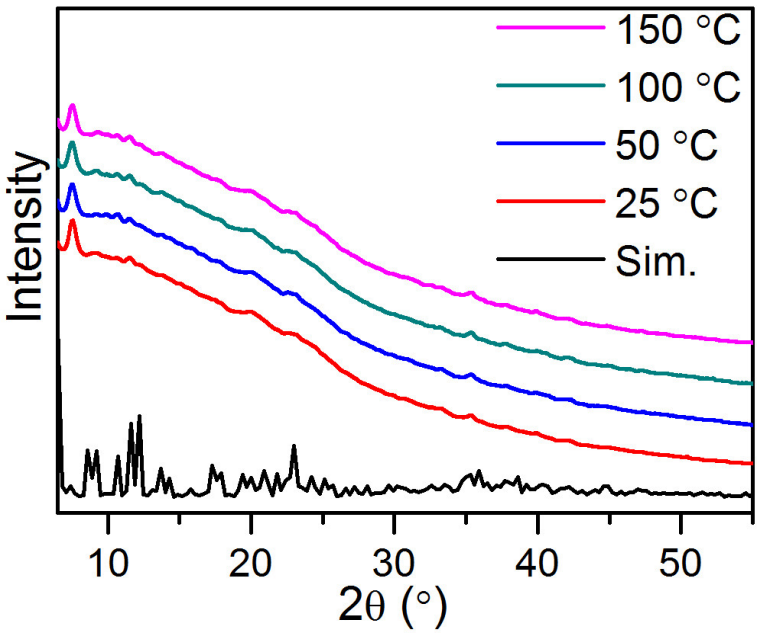

Figure S7. PXRD of **Ag_{14}–LR** from 25 °C to 150 °C.

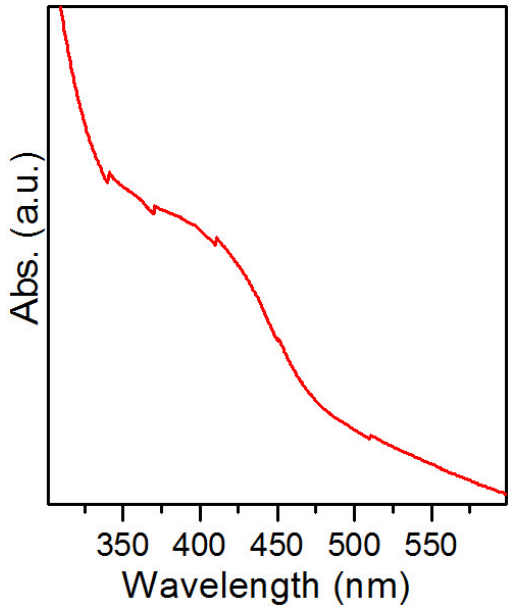

Figure S8. Solid state UV-vis spectrum of **Ag_{14}–LS** (crystals).

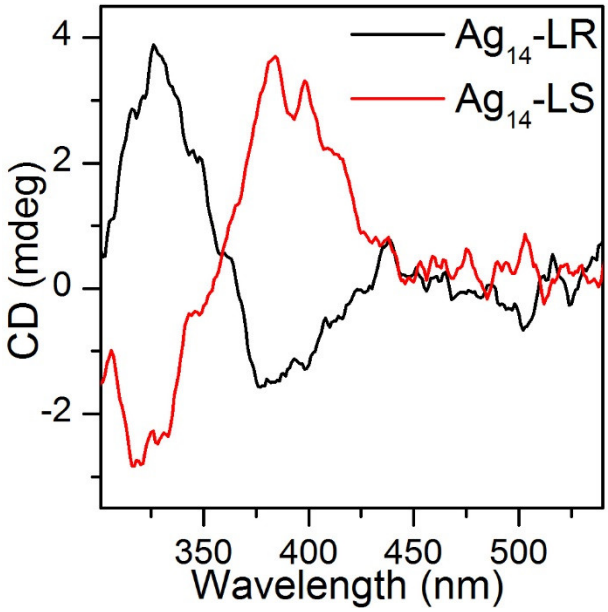

Figure S9. Solid state CD spectra of **Ag_{14}–LS** (crystals) and **Ag_{14}–LR** (crystals).

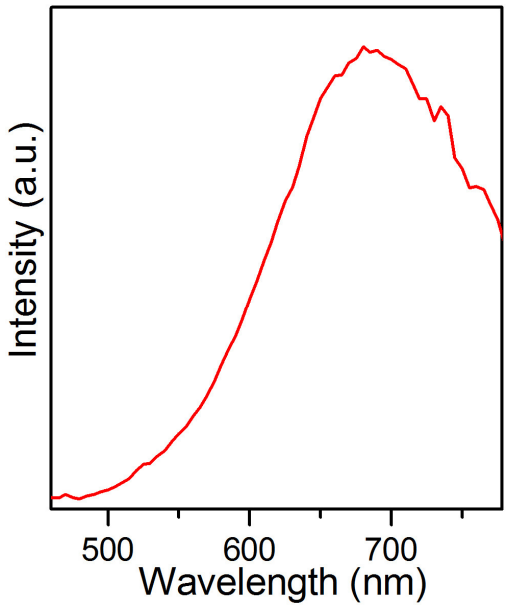

Figure S10. Solid-state fluorescence spectrum of **Ag_{14}-LR** at room temperature, excited at 420 nm.

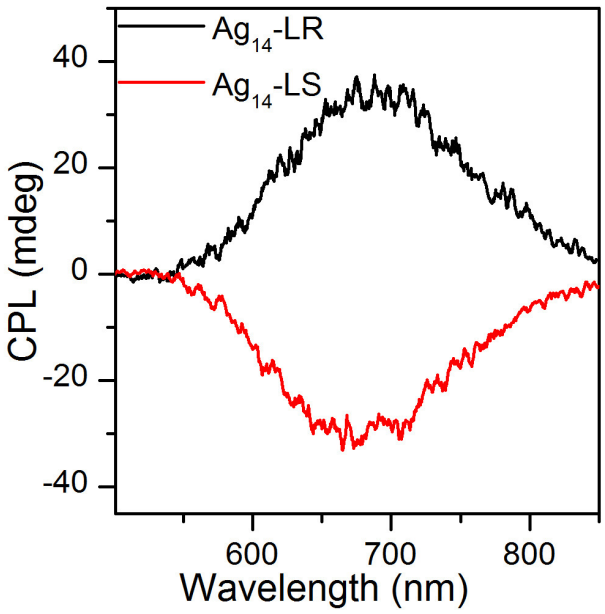

Figure S11. Solid-state CPL spectra of the **Ag14-LR/LS** enantiomers.

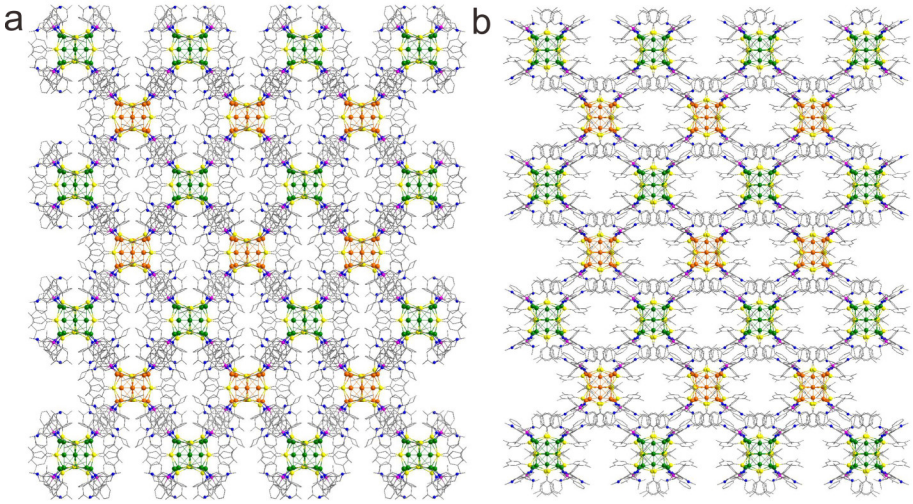

Figure S12. Crystal structure of **Ag14–LRS** viewed along *c* (a) and *b* axis (b). Color legend: orange and green sphere, Ag; yellow sphere, S; pink sphere, P; blue sphere, N; grey sphere, C. All hydrogen and fluorine atoms are omitted for clarity.

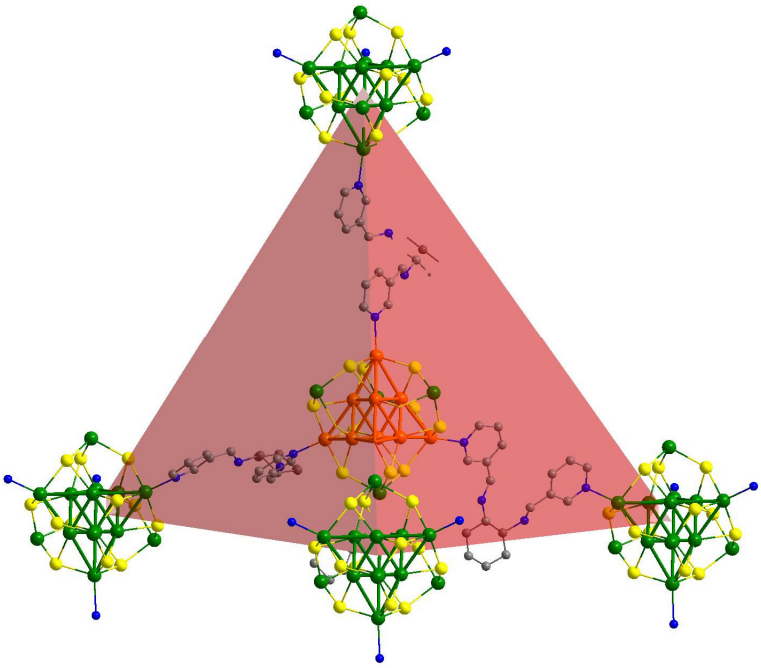

Figure S13. Regular tetrahedron structure formed by the **Ag_{14}** building blocks (as nodes) in **Ag_{14}-LRS**. Color legend: orange and green sphere, Ag; yellow sphere, S; blue sphere, N; grey sphere, C.

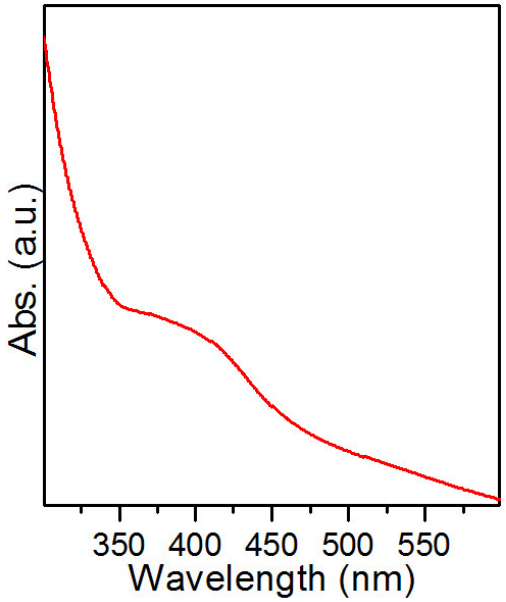

Figure S14. Solid state UV-vis spectrum of **Ag_{14}–LRS** (crystals).

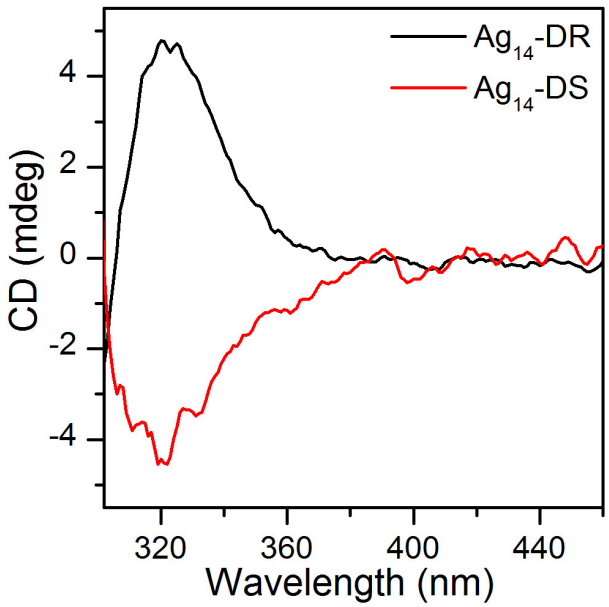

Figure S15. CD spectra of **Ag14–DR** and **Ag14–DS** in dichloromethane, DMF and methanol mixed solution (1.0 : 0.05 : 0.1).

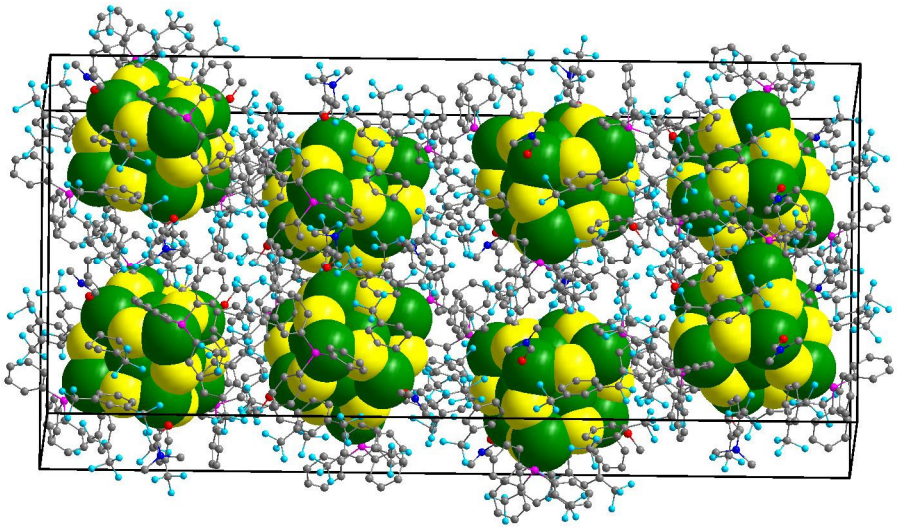

Figure S16. The packing diagram of **R-Ag14m**. Colour legend: green sphere, Ag; yellow sphere, S; pink sphere, P; red sphere, O; blue sphere, N; sky blue sphere, F; grey sphere, C. All hydrogen atoms are omitted for clarity.

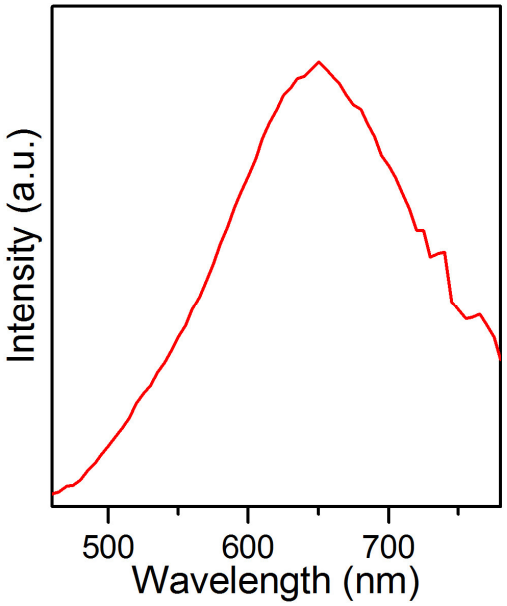

Figure S17. Solid-state fluorescence spectrum of **R-Ag$_{14m}$** at room temperature, excited at 420 nm.

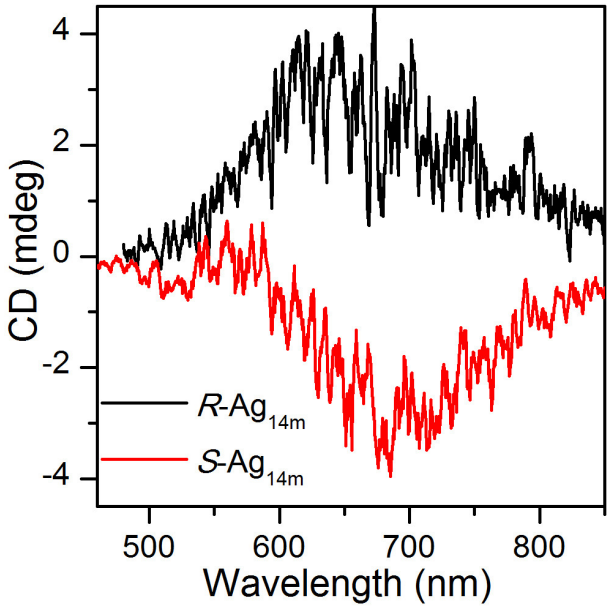

Figure S18. Solid-state CPL spectra of the **R/S-Ag$_{14m}$** enantiomers.

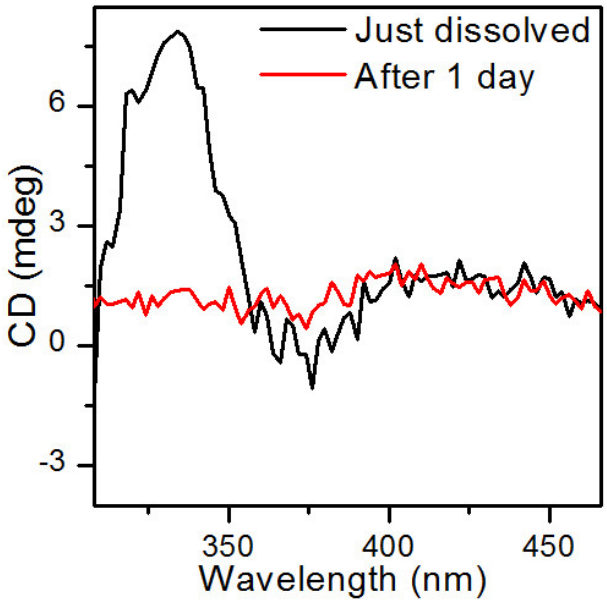

Figure S19. Comparison of the CD spectra of the **R-Ag$_{14m}$** crystals just dissolved in DMF and after 1 day at room temperature.

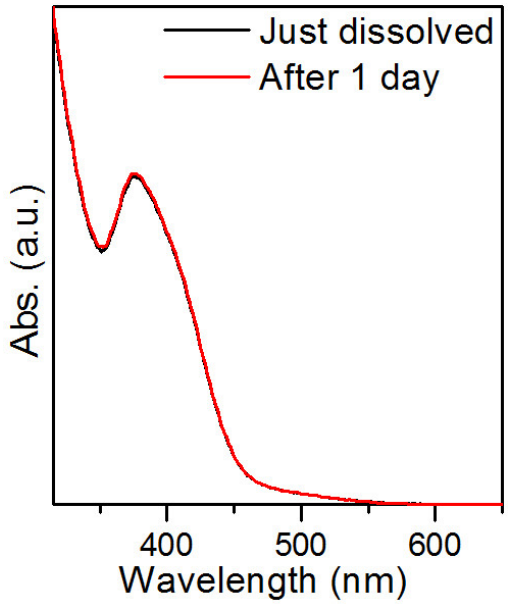

Figure S20. Comparison of the UV-vis spectra of the **R-Ag$_{14m}$** crystals just dissolved in DMF and after 1 day at room temperature.

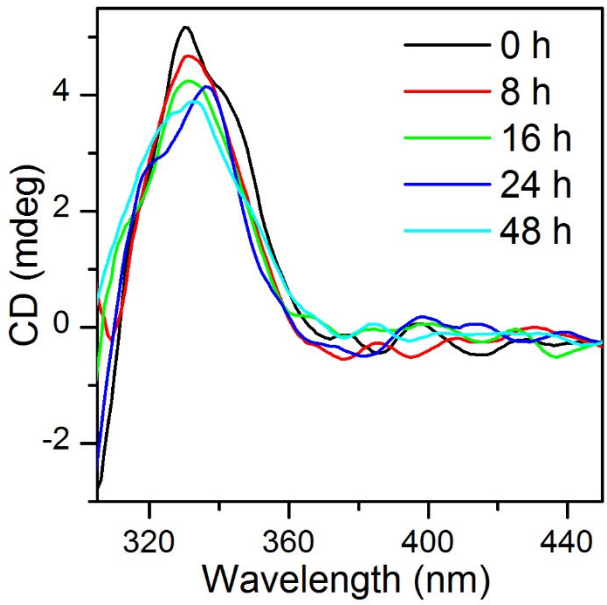

Figure S21. The intensity changes of the CD spectra of **Ag$_{14}$–DR** in dichloromethane, DMF and methanol mixed solution (1.0 : 0.05 : 0.1) with times at different 25 °C.

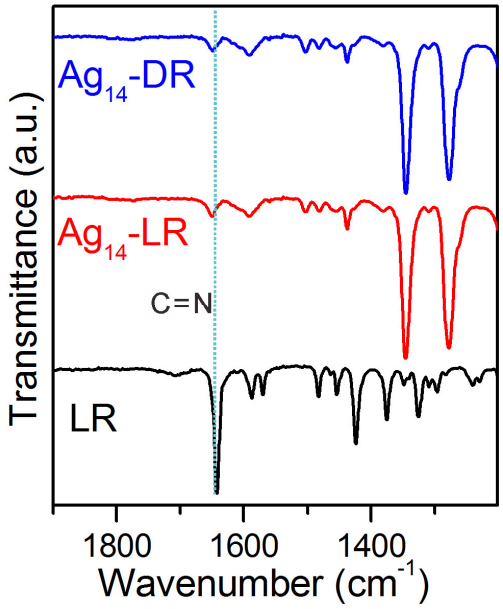

Figure S22. Solid-state FT-IR spectra of **Ag$_{14}$–DR**, crystals of **Ag$_{14}$–LR** and **LR**.

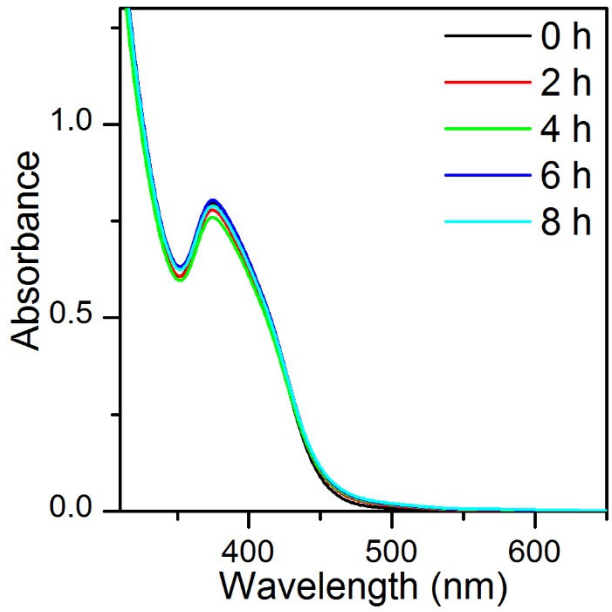

Figure S23. UV-vis spectra of pure **R-Ag$_{14m}$** crystals dissolved in DMF during racemization at 30 °C.

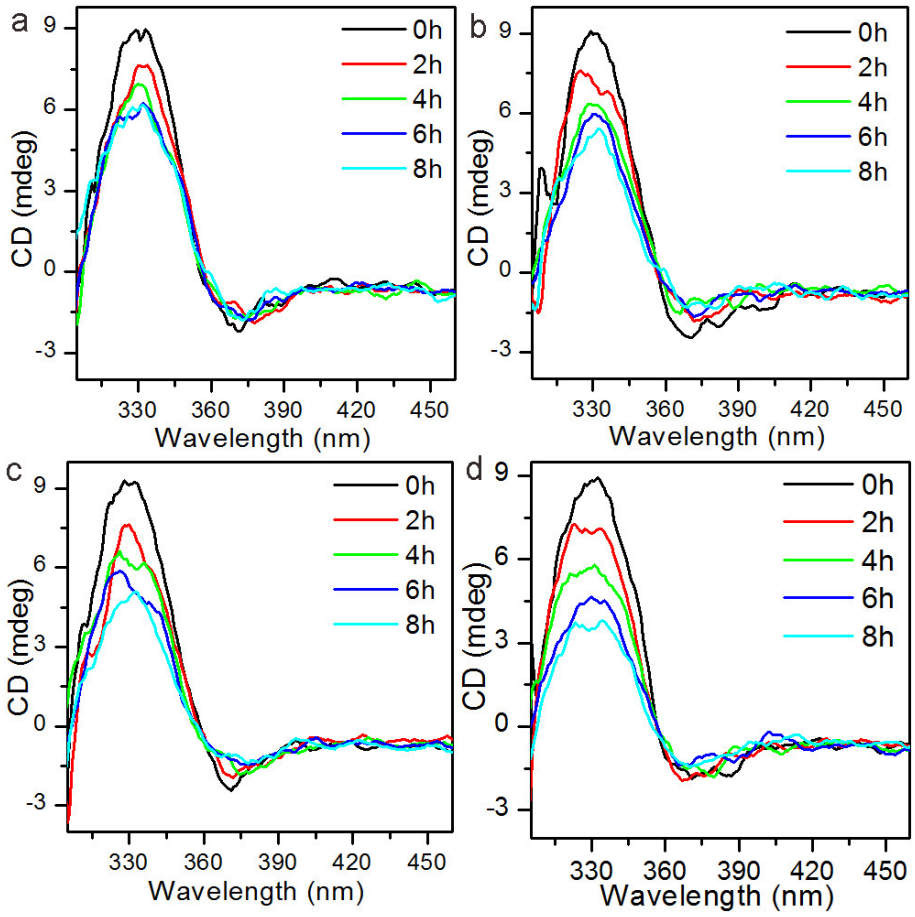

Figure S24. The intensity changes of the CD spectra of **R-Ag$_{14m}$** crystals in DMF with times at different temperatures: (a) 0 °C; (b) 10 °C; (c) 20 °C; (d) 30 °C.

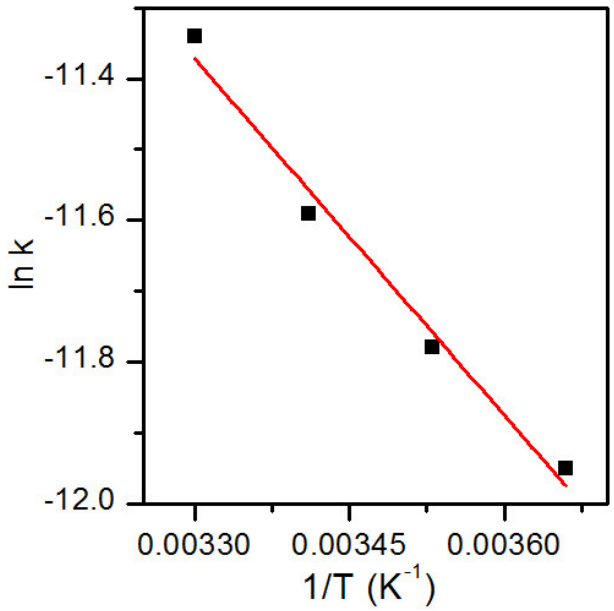

Figure S25. Arrhenius plot ln(*k*) vs 1/T for the auto-racemization of pure crystals of **R-Ag$_{14m}$**.

Table S1. Crystal data and structure refinement for **Ag_{14}-LR.**

Identification code	**Ag_{14}-LR**
Empirical formula	$C_{204}H_{136}Ag_{14}F_{72}N_8P_4S_{12}$
Formula weight	6085.98
Temperature/K	100.01(10)
Crystal system	hexagonal
Space group	$P6_122$
a/Å	23.6655(7)
b/Å	23.6655(7)
c/Å	81.7805(17)
α/°	90
β/°	90
γ/°	120
Volume/Å^3	39665(2)
Z	6
ρ_{calc}g/cm^3	1.529
μ/mm^{-1}	10.069
F(000)	17844.0
Crystal size/mm^3	0.02 × 0.01 × 0.01
Radiation	Cu Kα (λ = 1.54184)
2Θ range for data collection/°	6.914 to 122.338
Index ranges	$-16 \leq h \leq 24$, $-21 \leq k \leq 18$, $-88 \leq l \leq 92$
Reflections collected	77560
Independent reflections	19620 [R_{int} = 0.1399, R_{sigma} = 0.1315]
Data/restraints/parameters	19620/1564/1355
Goodness-of-fit on F^2	1.042
Final R indexes [I>=2σ (I)]	R_1 = 0.1023, wR_2 = 0.2235
Final R indexes [all data]	R_1 = 0.1265, wR_2 = 0.2442
Largest diff. peak/hole / e Å^{-3}	1.51/-1.67
Flack parameter	0.018(8)

Table S2. Crystal data and structure refinement for **Ag_{14}-LS.**

Identification code	**Ag_{14}-LS**
Empirical formula	$C_{204}H_{136}Ag_{14}F_{72}N_8P_4S_{12}$
Formula weight	6085.98
Temperature/K	100.01(10)
Crystal system	hexagonal
Space group	$P6_522$
a/Å	23.6036(4)
b/Å	23.6036(4)
c/Å	80.9175(11)
α/°	90
β/°	90
γ/°	120
Volume/Å^3	39041.8(14)
Z	6
ρ_{calc}g/cm^3	1.553
μ/mm^{-1}	10.229
F(000)	17844.0
Crystal size/mm^3	0.03 × 0.02 × 0.02
Radiation	Cu Kα (λ = 1.54184)
2Θ range for data collection/°	6.966 to 122.338
Index ranges	$-26 \leq h \leq 26$, $-26 \leq k \leq 26$, $-91 \leq l \leq 91$
Reflections collected	156944
Independent reflections	20006 [R_{int} = 0.1401, R_{sigma} = 0.0703]
Data/restraints/parameters	20006/1002/1415
Goodness-of-fit on F^2	1.069
Final R indexes [I>=2σ (I)]	R_1 = 0.0892, wR_2 = 0.1872
Final R indexes [all data]	R_1 = 0.1013, wR_2 = 0.1959
Largest diff. peak/hole / e Å^{-3}	1.40/-1.13
Flack parameter	0.055(5)

Table S3. Crystal data and structure refinement for **Ag_{14}-LRS.**

Identification code	**Ag_{14}-LRS**
Empirical formula	$C_{204}H_{136}Ag_{14}F_{72}N_8P_4S_{12}$
Formula weight	6085.98
Temperature/K	100.00(10)
Crystal system	orthorhombic
Space group	Pnnn
a/Å	20.4683(3)
b/Å	24.1337(4)
c/Å	25.9145(6)
α/°	90
β/°	90
γ/°	90
Volume/Å^3	12801.1(4)
Z	2
ρ_{calc}g/cm^3	1.579
μ/mm^{-1}	10.400
F(000)	5948.0
Crystal size/mm^3	0.02 × 0.01 × 0.01
Radiation	Cu Kα (λ = 1.54184)
2Θ range for data collection/°	7.326 to 122.338
Index ranges	$-23 \leq h \leq 20$, $-27 \leq k \leq 20$, $-27 \leq l \leq 29$
Reflections collected	38362
Independent reflections	9835 [R_{int} = 0.0693, R_{sigma} = 0.0529]
Data/restraints/parameters	9835/752/784
Goodness-of-fit on F^2	1.017
Final R indexes [I>=2σ (I)]	R_1 = 0.0616, wR_2 = 0.1627
Final R indexes [all data]	R_1 = 0.0909, wR_2 = 0.1930
Largest diff. peak/hole / e Å^{-3}	1.63/-1.00

Table S4. Crystal data and structure refinement for **R-Ag$_{14m}$**.

Identification code	**R-Ag$_{14m}$**
Empirical formula	$C_{178}H_{121}Ag_{14}F_{72}N_3O_4P_4S_{12}$
Formula weight	5752.55
Temperature/K	100.01(10)
Crystal system	orthorhombic
Space group	$C222_1$
a/Å	24.9972(3)
b/Å	30.3589(4)
c/Å	56.1233(7)
α/°	90
β/°	90
γ/°	90
Volume/Å^3	42591.3(9)
Z	8
ρ_{calc}g/cm^3	1.794
μ/mm^{-1}	12.465
F(000)	22400.0
Crystal size/mm^3	0.05 × 0.02 × 0.02
Radiation	Cu Kα (λ = 1.54184)
2Θ range for data collection/°	6.58 to 122.338
Index ranges	-25 ≤ h ≤ 28, -34 ≤ k ≤ 34, -63 ≤ l ≤ 63
Reflections collected	129060
Independent reflections	32755 [R_{int} = 0.1137, R_{sigma} = 0.0904]
Data/restraints/parameters	32755/1869/2570
Goodness-of-fit on F^2	1.058
Final R indexes [I>=2σ (I)]	R_1 = 0.0790, wR_2 = 0.1977
Final R indexes [all data]	R_1 = 0.0944, wR_2 = 0.2110
Largest diff. peak/hole / e Å^{-3}	1.92/-1.29
Flack parameter	-0.026(5)

Table S5. Crystal data and structure refinement for **S-Ag$_{14m}$**.

Identification code	**S-Ag$_{14m}$**
Empirical formula	$C_{178}H_{121}Ag_{14}F_{72}N_3O_4P_4S_{12}$
Formula weight	5752.55
Temperature/K	100.01(10)
Crystal system	orthorhombic
Space group	$C222_1$
a/Å	24.8562(2)
b/Å	30.5304(3)
c/Å	56.0821(5)
α/°	90
β/°	90
γ/°	90
Volume/Å^3	42559.1(7)
Z	8
ρ_{calc}g/cm^3	1.796
μ/mm^{-1}	12.475
F(000)	22400.0
Crystal size/mm^3	0.04 × 0.02 × 0.02
Radiation	Cu Kα (λ = 1.54184)
2Θ range for data collection/°	6.586 to 122.334
Index ranges	-28 ≤ h ≤ 16, -34 ≤ k ≤ 33, -63 ≤ l ≤ 48
Reflections collected	69042
Independent reflections	32631 [R_{int} = 0.0594, R_{sigma} = 0.0606]
Data/restraints/parameters	32631/1935/2557
Goodness-of-fit on F^2	1.057
Final R indexes [I>=2σ (I)]	R_1 = 0.0692, wR_2 = 0.1759
Final R indexes [all data]	R_1 = 0.0712, wR_2 = 0.1776
Largest diff. peak/hole / e Å^{-3}	2.21/-2.33
Flack parameter	0.015(5)